BBA - Molecular Basis of Disease 1865 (2019) 1525–1539

Contents lists available at ScienceDirect

BBA - Molecular Basis of Disease

journal homepage: www.elsevier.com/locate/bbadis

# Pinealectomy or light exposure exacerbates biliary damage and liver fibrosis in cholestatic rats through decreased melatonin synthesis

Lixian Chen[b,k], Tianhao Zhou[b], Nan Wu[b,1], April O'Brien[b], Julie Venter[b,1], Ludovica Ceci[b,1], Konstantina Kyritsi[b,1], Paolo Onori[e], Eugenio Gaudio[e], Amelia Sybenga[f], Linglin Xie[g], Chaodong Wu[g], Luca Fabris[h,i], Pietro Invernizzi[j,2], David Zawieja[b], Suthat Liangpunsakul[c,d], Fanyin Meng[a,b,1], Heather Francis[a,b,1], Gianfranco Alpini[a,b,1,3], Qiaobing Huang[k,3], Shannon Glaser[b,*,3]

[a] Research, Central Texas Veterans Health Care System, United States of America
[b] Department of Medical Physiology, Texas A&M University, College of Medicine, United States of America
[c] Richard L. Roudebush VA Medical Center, Research, United States of America
[d] Indiana University, Gastroenterology, Medicine, United States of America
[e] Department of Anatomical, Histological, Forensic Medicine and Orthopedics Sciences, Sapienza University of Rome, Rome, Italy
[f] Department of Pathology, Microbiology and Immunology, Vanderbilt University School of Medicine, Nashville, TN, United States of America
[g] Department of Nutrition and Food Science, Texas A&M University, College Station, TX, United States of America
[h] Department of Molecular Medicine, University of Padua School of Medicine, Padua, Italy
[i] Digestive Disease Section, Yale University School of Medicine, New Haven, CT, United States of America
[j] Humanitas Clinical and Research Center, Rozzano, Milan, Italy
[k] Department of Pathophysiology, Key Lab for Shock and Microcirculation Research of Guangdong Province, Southern Medical University, Guangzhou, PR China

ARTICLE INFO

*Keywords:*
Arylalkylamine *N*-acetyltransferase
Clock genes
Melatonin receptors
Reactive oxygen species
Senescence

ABSTRACT

Melatonin, a neuroendocrine hormone synthesized by the pineal gland and cholangiocytes, decreases biliary hyperplasia and liver fibrosis during cholestasis-induced biliary injury via melatonin-dependent autocrine signaling through increased biliary arylalkylamine *N*-acetyltransferase (AANAT) expression and melatonin secretion, downregulation of miR-200b and specific circadian clock genes. Melatonin synthesis is decreased by pinealectomy (PINX) or chronic exposure to light. We evaluated the effect of PINX or prolonged light exposure on melatonin-dependent modulation of biliary damage/ductular reaction/liver fibrosis. Studies were performed in male rats with/without BDL for 1 week with 12:12 h dark/light cycles, continuous light or after 1 week of PINX. The expression of AANAT and melatonin levels in serum and cholangiocyte supernatant were increased in BDL rats, while decreased in BDL rats following PINX or continuous light exposure. BDL-induced increase in serum chemistry, ductular reaction, liver fibrosis, inflammation, angiogenesis and ROS generation were significantly enhanced by PINX or light exposure. Concomitant with enhanced liver fibrosis, we observed increased biliary senescence and enhanced clock genes and miR-200b expression in total liver and cholangiocytes. In vitro,

*Abbreviations:* AANAT, arylalkylamine *N*-acetyltransferase; ALP, alkaline phosphatase; ARNTL, aryhydrocarbon receptor nuclear translocator-like protein 1; α–SMA, alpha-smooth muscle actin; BDL, bile duct ligation; CCL2, C-C motif chemokine ligand 2; CK-19, cytokeratin-19; CLOCK, circadian locomotor output cycles kaput; Col1a1, collagen type I alpha 1; Cry1, Cryptochromes 1; Fn1, fibronectin 1; GAPDH, glyceraldehyde-3-phosphate dehydrogenase; H&E, hematoxylin & eosin; HSCs, hepatic stellate cells; HHStecs, human hepatic stellate cell lines; IBDM, intrahepatic bile duct mass; IL, interleukin; LCM, laser capture microdissection; MT1, melatonin receptor 1A; MT2, melatonin receptor 1B; PINX, pinealectomy; p16 (Cdkn2a), cyclin-dependent kinase inhibitor 2A; p21 (Cdkn1a), cyclin-dependent kinase inhibitor 1A; PBC, primary biliary cholangitis; PCNA, proliferating cell nuclear antigen; Per1, period circadian protein homolog 1; PECAM-1, platelet endothelial cell adhesion molecule 1; PSC, primary sclerosing cholangitis; ROS, reactive oxygen species; SA-β-gal, senescence associated β galactosidase; SGTP, alanine aminotransferase; SGOT, aspartate aminotransferase; TGF-β1, transforming growth factor-beta 1; TGF-βR1, transforming growth factor-beta receptor 1; VEGFA, vascular endothelial growth factor A; vWF, Von Willebrand Factor; WT, wild-type

* Corresponding author at: Department of Medical Physiology, Texas A&M University College of Medicine, 702 SW HK Dodgen Loop, Temple, TX 76504, United States of America.
*E-mail address:* sglaser@medicine.tamhsc.edu (S. Glaser).
[1] Present address: Richard L. Roudebush VA Medical Center, Research, and Indiana University, Gastroenterology, Medicine, Indianapolis, Indiana.
[2] Present address: Division of Gastroenterology and Center for Autoimmune Liver Diseases, San Gerardo Hospital, Department of Medicine and Surgery, University of Milan-Bicocca, Monza, Italy.
[3] Drs. Alpini, Huang and Glaser share senior authorship.

https://doi.org/10.1016/j.bbadis.2019.03.002
Received 26 January 2019; Received in revised form 11 March 2019; Accepted 14 March 2019
Available online 16 March 2019

the expression of AANAT, clock genes and miR-200b was increased in PSC human cholangiocyte cell lines (hPSCL). The proliferation and activation of HHStecs (human hepatic stellate cell lines) were increased after stimulating with BDL cholangiocyte supernatant and further enhanced when stimulated with BDL rats following PINX or continuous light exposure cholangiocyte supernatant via intracellular ROS generation. Conclusion: Melatonin plays an important role in the protection of liver against cholestasis-induced damage and ductular reaction.

## 1. Introduction

Melatonin, a neuroendocrine hormone synthesized by the pineal gland and cholangiocytes, inhibits biliary hyperplasia and liver fibrosis during cholestatic injury by an autocrine pathway though: (i) upregulation of arylalkylamine *N*-acetyltransferase (AANAT, the enzyme regulating melatonin synthesis) and melatonin secretion; and (ii) downregulation of clock genes (CLOCK, ARNTL, Cry1, and Per1) [1,2]. The levels of melatonin are reduced by pinealectomy (PINX) [3] and exposure to light but increased by dark exposure, detected by the photosensitive ganglion cells of the retina [4], however no information exists on the role of PINX on biliary functions.

Cholangiocytes undergo senescence in human cholangiopathies including primary sclerosing cholangitis (PSC) and primary biliary cholangitis (PBC) [5] and animal models of cholestasis including bile duct ligation (BDL) and the Mdr2$^{-/-}$ mouse model that mimics some features of PSC [6,7]. Release of SASPs (senescence associated secretory phenotypes) during biliary senescence represents an important pathogenic mechanism in cholangiopathies including PSC [8] that cause paracrine activation of hepatic stellate cells with subsequent enhanced liver fibrosis [8,9].

Melatonin ameliorates liver damage by attenuating oxidative stress, inflammatory responses in animal models of hepatic cirrhosis and fibrosis [10–12]. We have previously shown that melatonin decreases biliary senescence and liver fibrosis of Mdr2$^{-/-}$ mice by downregulating miR-200b-dependent liver angiogenesis [13]. PINX aggravates acute caerulein-induced pancreatitis, which is related to reduce melatonin levels in pancreas of animals with PINX [14]. Since no data exists regarding the role of central regulation of melatonin synthesis in cholangiopathies, we evaluated the effect of PINX or light exposure on melatonin-dependent modulation of biliary damage and liver fibrosis.

## 2. Materials and methods

### 2.1. Materials

Reagents were purchased from Sigma-Aldrich (St. Louis, MO) unless otherwise indicated. The antibodies for cytokeratin-19 (CK-19, ab 52625), AANAT (ab3505), MT1 (ab203038), MT2 (ab203346), cyclin-dependent kinase inhibitor 1A (p16, ab189043), CLOCK (ab3517), desmin (ab185033) and CD68 (ab31630) were purchased from Abcam (Cambridge, MA); mouse CK-19 antibody (NCL-LCK19) was purchased from Leica (Buffalo Grove, IL); MT1(sc390328, sc390328AF488) from mouse and hepatocyte nuclear factor-4α (HNF-4α, sc6556) were purchased from Santa Cruz (Dallas, TX); CD31 (AF3628) was purchased from R&D Systems Inc. (Minneapolis, MN). Commercially available enzyme-linked immunosorbent assay (ELISA) kits for measuring melatonin levels in serum and biliary supernatant were purchased from Genway (San Diego, CA). ELISA kits to measure transforming growth factor-β1 (TGF-β1) levels were purchased from Affymetrix Inc. (Santa Clara, CA). Reactive oxygen species (ROS) detection assay kits for measuring ROS levels were purchased from Cell Biolabs, Inc. (San Diego, CA) and Abcam. MTS Cell Titer 96 Aqueous One Solution Reagent assay kit was purchased from Promega Corporation (Madison, WI, USA). The RNeasy Mini Kit for RNA purification and the selected primers were purchased from Qiagen (Valencia, CA). The iScript cDNA Synthesis Kit (170-8891) and iTaq Universal SYBR Green Supermix (172-5124) were purchased from Bio-Rad (Hercules, CA). The information of real-time PCR (*q*PCR) primers used in this project is listed in Supplemental Table 1.

### 2.2. Animal models

Animal experiments were performed according to protocols approved by the Baylor Scott & White Research Institute CTX IACUC. Male Fischer 344 rats (200–225 g) were purchased from Charles River (Wilmington, MA) and housed in a temperature-controlled environment (22 °C). The PINX surgery [15] was performed by Charles River according to a surgical procedure approved by their Animal Use Protocol (AUP). Briefly, the animals were placed in the stereotaxic apparatus and skin incision was made. A hole was drilled into the skull to access the pineal gland. The venous sinuses were ligated and the pineal gland was removed. The skin incision was closed with wound clips. Seven days after PINX, rats underwent sham or BDL for 1 week [16] at the Baylor Scott Animal Facility. In separate experiments, normal and BDL rats (immediately after surgery) were housed in 12:12 h light-dark cycles or complete light for 1 week. In all groups, liver and body weight and liver to body weight ratio were measured; serum, total liver samples, cholangiocytes, cholangiocyte supernatant and selected organs were also collected.

Since melatonin treatment or dark therapy (that increases melatonin serum levels) [13] decreases biliary damage and liver fibrosis through downregulation of miR-200b, the expression of selected clock genes was measured in: (i) normal wild-type (WT, FVB/NJ, 12 wk. age) mice (Jackson Laboratories, Ann Harbor, MN); (ii) Mdr2$^{-/-}$ (Abcb4) control mice; and (iii) Mdr2$^{-/-}$ mice (12 wk. age) treated with melatonin in drinking water (20 mg/L corresponding to a melatonin intake of 2 mg/Kg BW/day) for 1 wk., Vivo-Morpholino sequences of miR-200b (5′-TCCAATGCTGCCCAGTAAGATGGCC-3-, to reduce the hepatic expression of miR-200b) or mismatched Morpholino (5′-TCCAATcCTcCCCAcTAAcATcGCC-3′) (Gene Tools, Philomath, OR) by 2 tail vein injections (at days 3 and 7, 30 mg/kg BW) [13] for 1 wk. Since in a preliminary study we have shown that in MT2$^{-/-}$ BDL mice there is enhanced biliary mass and liver fibrosis [17], we treated normal and BDL rats (immediately after surgery) with melatonin in drinking water (20 mg/L corresponding to a melatonin intake of 2 mg/Kg BW/day) for 1 wk. before measuring changes in biliary mass and liver fibrosis.

### 2.3. Human healthy control and PSC samples

The liver tissue samples (paraffin-embedded sections) collected from healthy human (n = 4) and PSC patients (n = 5, diagnosed by a board-certified pathologist, Humanitas Clinical and Research Center, Rozzano, Italy) (Supplementary Table 2) were obtained from Dr. Pietro Invernizzi. The unidentified human samples were obtained under a protocol approved by the Ethics Committee of the Humanitas Research Hospital; the protocol was reviewed by the Veterans' Administration IRB and International Research Committee. Written informed consent was received from participants prior to inclusion in the study. The use of human tissue was approved by the Texas A&M HSC College of Medicine Institutional Review Board. The RNeasy was used to extract total RNA from paraffin-embedded liver sections.

### 2.4. Isolated cholangiocytes and HSCs

Cholangiocytes were obtained by immunoaffinity separation [18] using a rat $IgG_{2a}$ monoclonal antibody (Dr. R. Faris, Brown University, Providence, RI) against an unidentified antigen expressed by all cholangiocytes. Rat HSCs were isolated by laser capture microdissection (LCM) using an antibody against desmin. Following immunofluorescence, desmin-positive cells were dissected from the slides by the LCM system Leica LMD7000 (Buffalo Grove, IL). RNA from HSCs were extracted with the Arcturus PicoPure RNA isolation kit (Thermo Fisher Scientific, Mountain View, CA).

### 2.5. Measurement of AANAT, MT1 and MT2 expression, melatonin levels in serum and cholangiocyte supernatant

We measured the immunoreactivity of AANAT, MT1 and MT2 by: (i) immunofluorescence in frozen liver sections (6 μm thick) co-stained with CK-19, desmin (marker of HSCs) or HNF-4α (hepatocyte marker); and (ii) immunohistochemistry in paraffin-embedded liver sections (4 μm thick) from the selected groups of animals. We measured by *q*PCR the expression of: (i) AANAT in pineal gland and cholangiocytes; (ii) MT1 and MT2 in cholangiocytes; and (iii) melatonin levels in serum and cholangiocyte supernatant by commercially available ELISA kits.

### 2.6. Assessment of the histology of liver and other organs, serum chemistry and TGF- β 1 levels in serum and cholangiocyte supernatant, intrahepatic bile duct mass (IBDM), liver fibrosis and HSC activation

The histology of liver, pancreas, heart, spleen, lung, kidney, stomach, small and large intestine was evaluated in paraffin-embedded liver sections (4 μm thick) by H&E staining. Sections were evaluated in a blinded fashion by a board-certified pathologist. Serum levels of alanine aminotransferase (SGPT), aspartate aminotransferase (SGOT), alkaline phosphatase (ALP), and total bilirubin were measured by a Dimension RxL Max Integrated Chemistry system (Dade Behring Inc., Deerfield IL), Chemistry Department, Baylor Scott & White Health.

We evaluated IBDM by immunohistochemistry for CK-19 in paraffin-embedded liver sections (4 μm thick, 10 fields analyzed from three different samples from three animals). Sections were evaluated by Image Pro-analyzer software (Olympus, Tokyo, Japan). Liver fibrosis was measured in liver sections (4 μm thick) by Sirius Red staining (10 different fields were analyzed from three samples from three animals). Liver fibrosis was evaluated by measurement of hydroxyproline levels in total liver samples using the hydroxyproline Assay Kit. We also measured: (i) the mRNA expression of α-SMA, TGF-β1, TGF-βR1, collagen type I alpha 1 (Col1a1) and fibronectin 1 (Fn1) in total liver and cholangiocytes by *q*PCR; and (ii) TGF-β1 levels in serum and cholangiocyte supernatant by ELISA kits. We evaluated HSC proliferation/activation by (i) immunofluorescence in frozen liver sections (6 μm) co-stained with desmin and α-SMA (index of HSC activation) [19]; and (ii) measurement of mRNA expression for proliferating cell nuclear antigen (PCNA), Ki67, α-SMA and TGF-β1, Col1a1 and Fn1 in LCM-isolated HSC.

### 2.7. Measurement of cellular senescence, inflammatory and angiogenesis markers and ROS levels

Cellular senescence was evaluated by: (i) staining for senescence-associated beta-galactosidase (SA-β-gal) in frozen liver sections (10 μm thick) using a commercially available kit (Millipore Sigma, Billerica, MA); and (ii) immunofluorescence for p16 in frozen liver sections (6 μm thick) co-stained with CK-19; following staining, images were obtained using Leica AF 6000 Modular Systems. We measured the mRNA expression of the senescence markers, p16, p21 and CCL2, in cholangiocytes and p16 and p21 in HSCs by *q*PCR. The mRNA expression of the inflammatory markers, IL-1β, IL-6, IL-33, and tumor necrosis factor (TNF-α), was evaluated by *q*PCR in total liver. We analyzed the number of Kupffer cells in rat liver sections by staining CD68. Kupffer cell number was measured by Visiomorph software. We measured the expression of the angiogenesis markers vascular endothelial growth factor A (VEGFA), Von Willebrand Factor (vWF) and (PECAM-1 or CD31) in total liver by *q*PCR. We evaluated the immunoreactivity of the angiogenic factor, platelet endothelial cell adhesion molecule (PECAM-1 or CD31), by immunofluorescence in frozen liver sections (6 μm thick). ROS generation in total liver samples and cholangiocyte supernatant was measured by ROS detection assay kits.

### 2.8. Expression of clock genes and miR-200b

Since the expression of circadian rhythm and its related clock genes is mediated by melatonin released by the pineal gland and peripheral organs including the liver [1,20–22], we measured by *q*PCR the expression of the clock genes (CLOCK, Per1, Cry1, and ARNTL) in: (i) total liver and/or cholangiocytes from the selected groups of animals; and (ii) total liver from healthy human and patients with early and advanced stage of PSC (see Supplementary Table 2). CLOCK immunoreactivity evaluated by immunofluorescence in frozen liver sections (6 μm thick) co-stained with CK-19. To understand the mechanisms by which changes in melatonin secretion (decreased by PINX and exposure to light) [23,24] affect biliary damage and liver fibrosis, we measured by miRNA *q*PCR the biliary expression of miR-200b in cholangiocytes and total liver samples, whose expression is downregulated during melatonin inhibition of biliary damage and liver fibrosis in $Mdr2^{-/-}$ mice [13].

### 2.9. In vitro studies in normal and human PSC cell lines, human hepatic stellate cells (HHStecs) and immortalized murine cholangiocytes (IMCLs)

Studies were performed in: (i) normal human cholangiocyte lines (HIBEpiC); (ii) a human cholangiocyte cell line (hPSCL) from an unidentified 46-year old male patient with stage 4 PSC without cholangiocarcinoma [5]; purity of hPSCL was evaluated by CK19 immunofluorescence; and (iii) IMCLs and HHStecs; the immunoreactivity of MT1 and MT2 in HHStecs was measured by immunofluorescence. We evaluated the: (i) mRNA expression of MT1, MT2, AANAT, clock genes, miR-200b, fibrosis and senescent genes in HIBEpiC and hPSCL by *q*PCR; and (ii) immunoreactivity of MT1, AANAT and p16 in HIBEpiC and hPSCL by immunofluorescence. HHStecs were also treated with cholangiocyte supernatant from the mentioned animal groups before evaluating (i) proliferation by MTS assays and the mRNA expression of PCNA and Ki67; (ii) ROS levels in cells by ROS detection kits; and (iii) the mRNA expression of fibrosis and senescence genes by *q*PCR. In vitro studies, IMCLs were treated with melatonin ($10^{-1}$ M), miR-200b inhibitor or miR-200b mimic before evaluating the expression of miR-200b, TGF-β1, Col1a1, Fn1, p16, p21 and CCL2 by *q*PCR. All of these studies were performed in triplicate.

### 2.10. Statistical analysis

All data are expressed as the mean ± SEM. Differences between groups were analyzed by unpaired Student's *t*-test when two groups were analyzed and one-way ANOVA when more than two groups were analyzed, followed by an appropriate post hoc test. The level of significance was set at $P < 0.05$.

## 3. Results

### 3.1. Measurement of AANAT, MT1 and MT2 expression, melatonin levels in serum and cholangiocyte supernatant

Parallel to our previous study [2], the immunoreactivity of AANAT was mostly seen in intrahepatic cholangiocytes and upregulated after

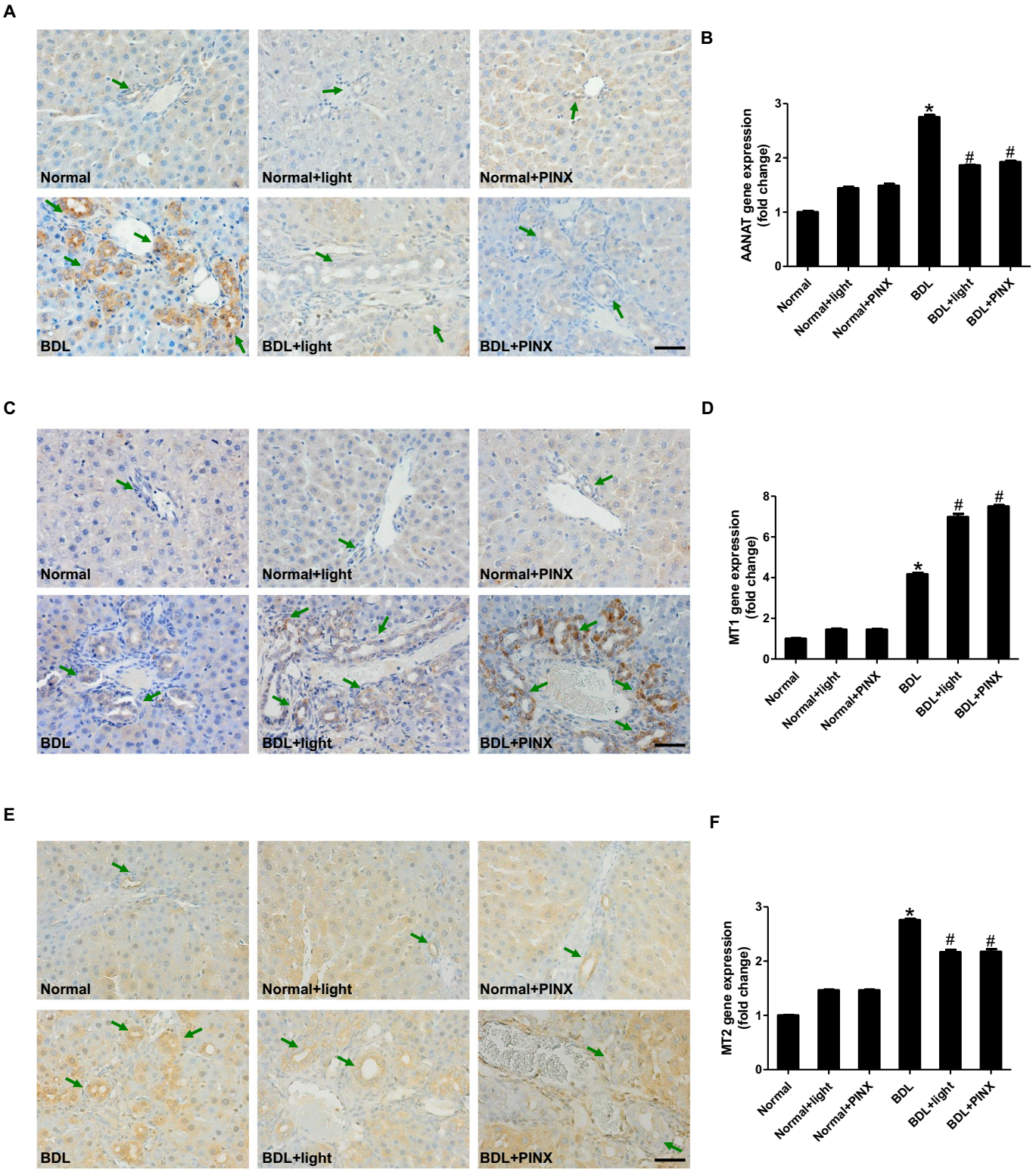


**Fig. 1.** [A–B] There were increased immunoreactivity [**A**] and mRNA expression in cholangiocytes [B] of AANAT in liver sections from BDL compared with normal rats, which were decreased in BDL rats with PINX or exposed to light [A–B] (Orig. magn., x40; scale bars 25 μm; green arrows indicate immunoreactivity of AANAT in cholangiocytes). [C–D] There were increased immunoreactivity [C] and mRNA expression in cholangiocytes [D] for MT1 in liver sections from BDL compared with normal rats, which were increased in BDL rats with PINX or exposed to light [C–D] (Orig. magn. ×40; scale bar 25 μm; green arrows indicate immunoreactivity of MT1 in cholangiocytes). [E–F] There were increased immunoreactivity [**E**] and mRNA expression in cholangiocytes [F] for MT2 in liver sections from BDL compared with normal rats, which were decreased in BDL rats with PINX or exposed to light compared with BDL rats [E–F] (Orig. magn. ×40; scale bar 25 μm; green arrows indicate immunoreactivity of MT1 in cholangiocytes). Data are mean ± SEM of 3 evaluations from 3 cumulative preparations of cholangiocytes from 4 rats.; $^{*}P < 0.05$ vs. Normal; $^{\#}P < 0.05$ vs. BDL.

BDL compared with normal rats; minimal immunoreactivity for AANAT was observed in BDL hepatocytes (Fig. 1A); no immunoreactivity for AANAT was observed in HSCs (Supplementary Fig. 1A). There was enhanced immunoreactivity of AANAT in cholangiocytes from BDL compared with normal rats (likely to a compensatory mechanism) [2], immunoreactivity that was decreased in BDL rats with PINX or exposed to light (Fig. 1A–B). AANAT mRNA expression was reduced in pineal glands of rats exposed to light compared with rats exposed to 12 h:12 h

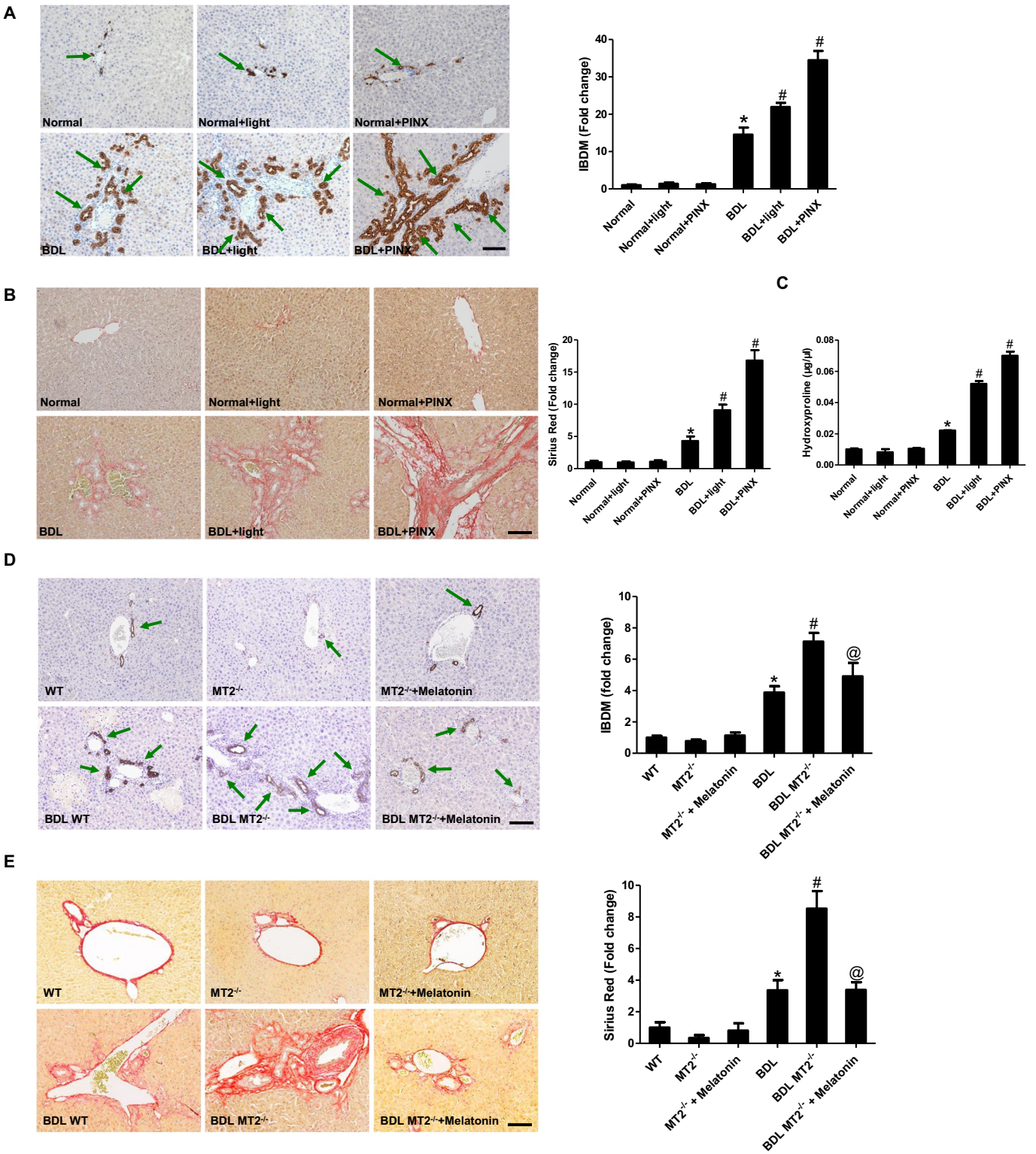


**Fig. 2.** [A] BDL-induced increases in IBDM in liver sections was further increased in BDL rats following PINX or exposed to light compared with BDL rats. [**B–C**] BDL-induced in collagen deposition in liver sections [B] and hydroxyproline levels in total liver [**C**] were further enhanced in BDL rats following PINX or exposed to light compared with BDL rats. [D–E] There were increased IBDM [D] and liver fibrosis [E] in BDL MT2$^{-/-}$ mice (compared with BDL mice) that were reduced by treatment with melatonin. Orig. magn. ×20; scale bar 50 μm. Data are mean ± SEM of: (i) 10 different fields analyzed from each sample from 3 different animals; and (ii) 3 evaluations from three total liver samples from 3 different rats $^{*}P < 0.05$ vs. Normal or WT; $^{\#}P < 0.05$ vs. BDL; $^{@}P < 0.05$ vs. BDL MT2$^{-/-}$.

light:dark cycles (Supplementary Fig. 1B). Melatonin levels were higher in serum and cholangiocyte supernatant from BDL compared with normal rats [2], but decreased in rats following PINX and exposed to light compared with rats exposed to 12 h:12 h light:dark cycles (Supplementary Fig. 1C).

The immunoreactivity of MT1 was mainly present in cholangiocytes (and at much lower extend in hepatocytes and HSCs) (Fig. 1C and E, and Supplementary Fig. 1D–F). The immunoreactivity of: (i) MT1 increased in cholangiocytes from BDL rats (compared with normal rats) and further increased in BDL rats with PINX or exposed to complete light compared with the respective control rats (Fig. 1C–D); and (ii) MT2 increased in cholangiocytes from BDL rats (compared with normal rats) but was decreased in BDL rats with PINX or prolonged light exposure compared with the respective control rats (Fig. 1E–F).

### 3.2. Assessment of the histology of liver and other organs, serum chemistry, TGF-β1 levels in serum and cholangiocyte supernatant, intrahepatic bile duct mass (IBDM) and liver fibrosis

By H&E staining we demonstrated: (i) moderate ductular reaction with bile stasis, minimally increased inflammation, Kupffer cell activation, ballooning degeneration and single hepatocyte necrosis in BDL rat liver; (ii) ductular reaction with bile stasis, minimal patchy active interface hepatitis and stage 2 fibrosis with focal early bridging (stage 3) in BDL rats exposed to light; and (iii) ductular reaction with bile stasis, mild patchy active interface hepatitis, focal stage 2 fibrosis with focal early bridging (stage 3), and collapse, markedly dilated portal veins in BDL rats following PINX (Supplementary Fig. 2A). However, there were no significant changes in the histology of the heart, spleen, kidney, small and large intestine and stomach between normal and BDL rats that underwent PINX or prolonged light exposure compared with their corresponding control rats (Supplementary Fig. 2B).

BDL-induced increases in: (i) serum levels of SGTP, SGOT, ALP and total bilirubin; and (ii) liver to body weight ratio were further increased in BDL rats following PINX or exposed to light compared with BDL rats (Table 1). BDL-induced increase in: (i) IBDM (Fig. 2A) and mRNA expression of PCNA and Ki67 in cholangiocytes (Supplementary Fig. 3A); (ii) liver fibrosis in liver sections (Fig. 2B) and total liver samples (Fig. 2C); (iii) mRNA expression of α-SMA, Col1a1, TGF-β1, TGF-βR1 and Fn1 in total liver samples (Supplementary Fig. 3B) and Col1a1, TGF-β1, TGF-βR1 and Fn1 in cholangiocytes (Supplementary Fig. 3C); and TGF-β1 levels in serum and cholangiocyte supernatant (Supplementary Fig. 3D) were further increased in BDL rats following PINX or exposed to light compared with BDL rats. In $MT2^{-/-}$ BDL mice, we demonstrated enhanced IBDM (Fig. 2D) and liver fibrosis (Fig. 2E) compared with BDL mice, parameters that were reduced by treatment of $MT2^{-/-}$ BDL mice with melatonin (Fig. 2D–E).

### 3.3. Evaluation of HSC proliferation and activation

By immunofluorescence, we observed increased expression of desmin and α-SMA in BDL compared with normal rats, expression that further enhanced in BDL rats following PINX or light treatment compared with BDL rats (Fig. 3A). We also observed enhanced mRNA expression of α-SMA, Col1a1, TGF-β1 and Fn1 (Fig. 3B), PCNA and Ki67 (Fig. 3C) in LCM-isolated HSC from BDL rats compared with normal rats, increases that were further enhanced in BDL rats following PINX or light treatment compared with LCM-isolated HSC from BDL rats (Fig. 3B–C).

### 3.4. Measurement of cellular senescence

There was enhanced cellular senescence (evidenced by SA-β-gal staining in liver sections from BDL compared with normal rats, Fig. 4A), which was further increased in BDL rats following PINX or light exposure compared with BDL rats (Fig. 4A). There was increased biliary immunoreactivity of p16 in BDL compared with normal rats, that was further increased in BDL rats following PINX or light treatment compared with BDL rats (Fig. 4B). The mRNA expression of p16, p21 and CCL2 was increased in cholangiocytes from BDL compared with normal rats and further enhanced in cholangiocytes from BDL rats following PINX or prolonged light exposure compared with BDL rats (Fig. 4C). However, there was decreased expression of the senescence markers, p16 and p21, in LCM-isolated HSC from BDL compared with normal rats, which was further decreased in BDL rats following PINX or light treatment compared with LCM-isolated HSC from BDL rats (Fig. 4D).

### 3.5. Evaluation of inflammatory, angiogenesis, and ROS levels

There was increased mRNA expression of: (i) IL-1β, IL-6, IL-33, and TNF-α (Fig. 5A); and (ii) VEGFA, vWF and PECAM-1 (Fig. 5C) in total liver samples from BDL compared with normal rats, expression that increased in total liver from BDL rats following PINX or light exposure compared with BDL rats. The immunoreactivity for CD68 (a marker of macrophages) [25] and CD31 (a marker of angiogenesis) [26] was enhanced in BDL compared with normal rats, and further increased in BDL rats following PINX or light exposure (Fig. 5B, D). ROS levels were increased in total liver (Fig. 5E) and cholangiocyte supernatant (Fig. 5F) from BDL compared with normal rats, and further increased in BDL rats following PINX or light exposure compared with BDL rats (Fig. 5E–F).

**Table 1**
Evaluation of serum levels of SGTP, SGOT, ALK PHOS and Total Bilirubin and liver to body weight ratio.

| Treatment | | Normal | Normal + light | Normal + PINX | BDL | BDL + light | BDL + PINX |
|---|---|---|---|---|---|---|---|
| Liver weight (gm) | | 5.05 ± 0.01 n = 4 | 6.53 ± 0.19 n = 4 | 7.31 ± 0.22 n = 4 | 7.22 ± 0.22 n = 4 | 7.09 ± 0.14 n = 4 | 9.36 ± 0.14 n = 4 |
| Body weight (gm) | | 123.7 ± 1.13 n = 4 | 153.0 ± 1.53 n = 4 | 171.8 ± 3.88 n = 4 | 148.5 ± 6.75 n = 4 | 129.3 ± 4.71 n = 4 | 172.1 ± 2.70 n = 4 |
| LW/BW (%) | | 4.09 ± 0.04 n = 4 | 4.27 ± 0.09 n = 4 | 4.26 ± 0.09 n = 4 | 4.87 ± 0.09* n = 4 | 5.47 ± 0.19# n = 4 | 5.45 ± 0.16# n = 4 |
| Serum chemistry | SGTP (units/L) | 165.5 ± 14.23 n = 4 | 163.2 ± 6.56 n = 4 | 151.5 ± 1.81 n = 4 | 254.5 ± 8.49* n = 4 | 300.0 ± 10.35# n = 4 | 357.8 ± 2.06# n = 4 |
| | SGOT (units/L) | 514.5 ± 58.89 n = 4 | 434.5 ± 46.33 n = 4 | 439.4 ± 6.67 n = 4 | 630.8 ± 46.2* n = 4 | 806.6 ± 38.96# n = 4 | 1332.5 ± 13.47# n = 4 |
| | ALK PHOS (units/L) | 332.9 ± 7.94 n = 4 | 307.00 ± 30.46 n = 4 | 296.1 ± 3.58 n = 4 | 403.3 ± 33.39* n = 4 | 479.2 ± 43.14# n = 4 | 589.0 ± 15.21# n = 4 |
| | Total bilirubin (mg/dL) | 0.6 ± 0.04 n = 4 | 0.6 ± 0.09 n = 4 | 0.53 ± 0.03 n = 4 | 6.88 ± 0.43* n = 4 | 8.23 ± 0.33# n = 4 | 9.77 ± 0.03# n = 4 |

* $P < 0.05$ vs. Normal.
# $P < 0.05$ vs. BDL.

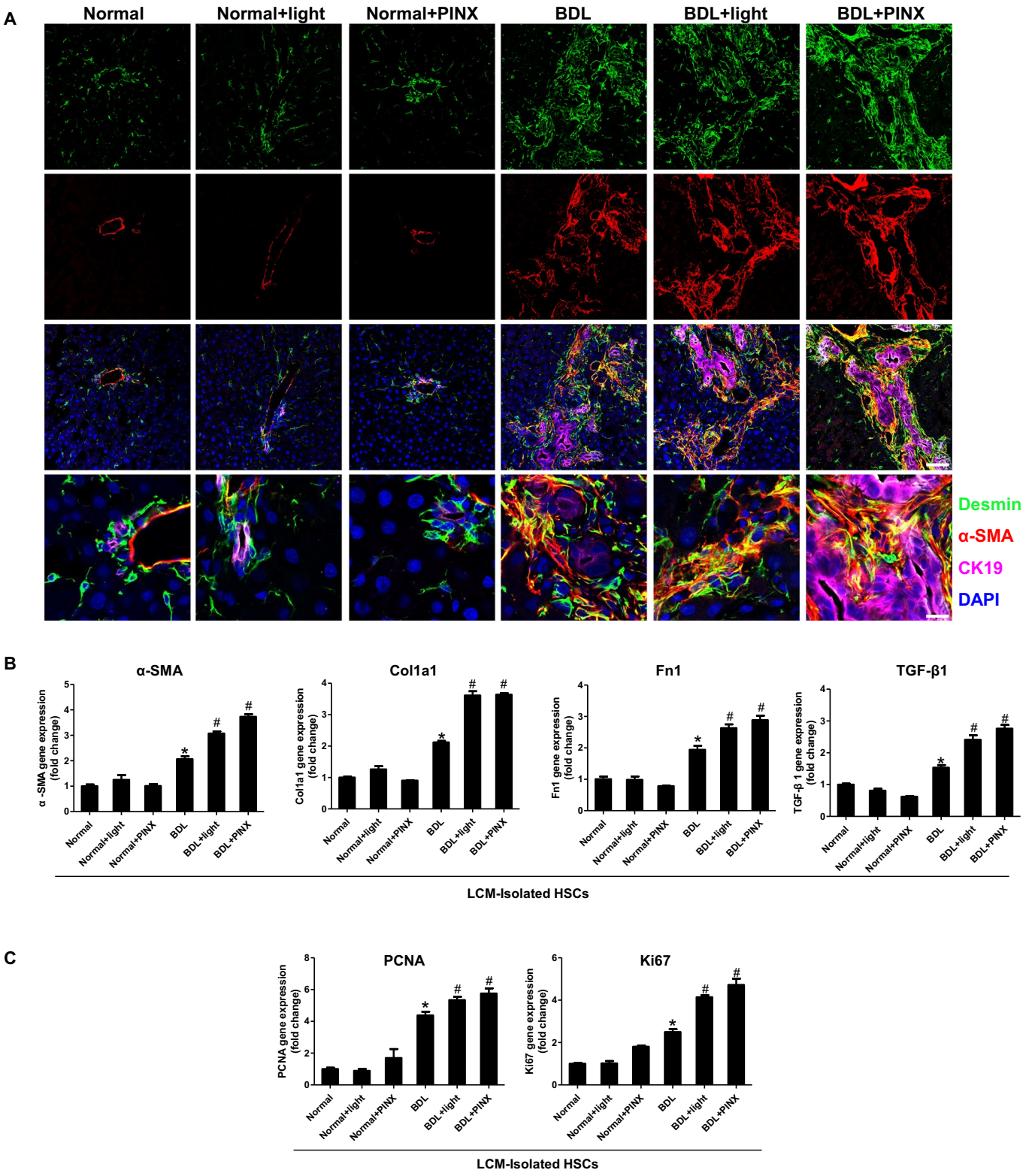


**Fig. 3.** [A] Immunofluorescence of liver sections co-stained CK19 (purple), desmin (green) and α-SMA (red) demonstrated increased for α-SMA and desmin in liver sections from BDL compared with normal rats, which was enhanced in liver sections from BDL rats following PINX or exposed to light (upper three panels: scale bar 50 μm; lower panel: scale bar 10 μm). [B] The expression of α-SMA, Col1a1, TGF-β1, and Fn1 increased in LCM isolated HSC from BDL compared with normal rats, which further increased in BDL rats following PINX or exposed to light compared with BDL rats. [C] There was increased expression of PCNA and Ki67 in LCM isolated HSC from BDL compared with normal rats, that was further increased in BDL rats following PINX or exposed to light compared with BDL rats. Data are mean ± SEM of 3 evaluations from 3 preparations LCM-isolated HSC from 3 rats. $^{*}P < 0.05$ vs. Normal; $^{\#}P < 0.05$ vs. BDL.

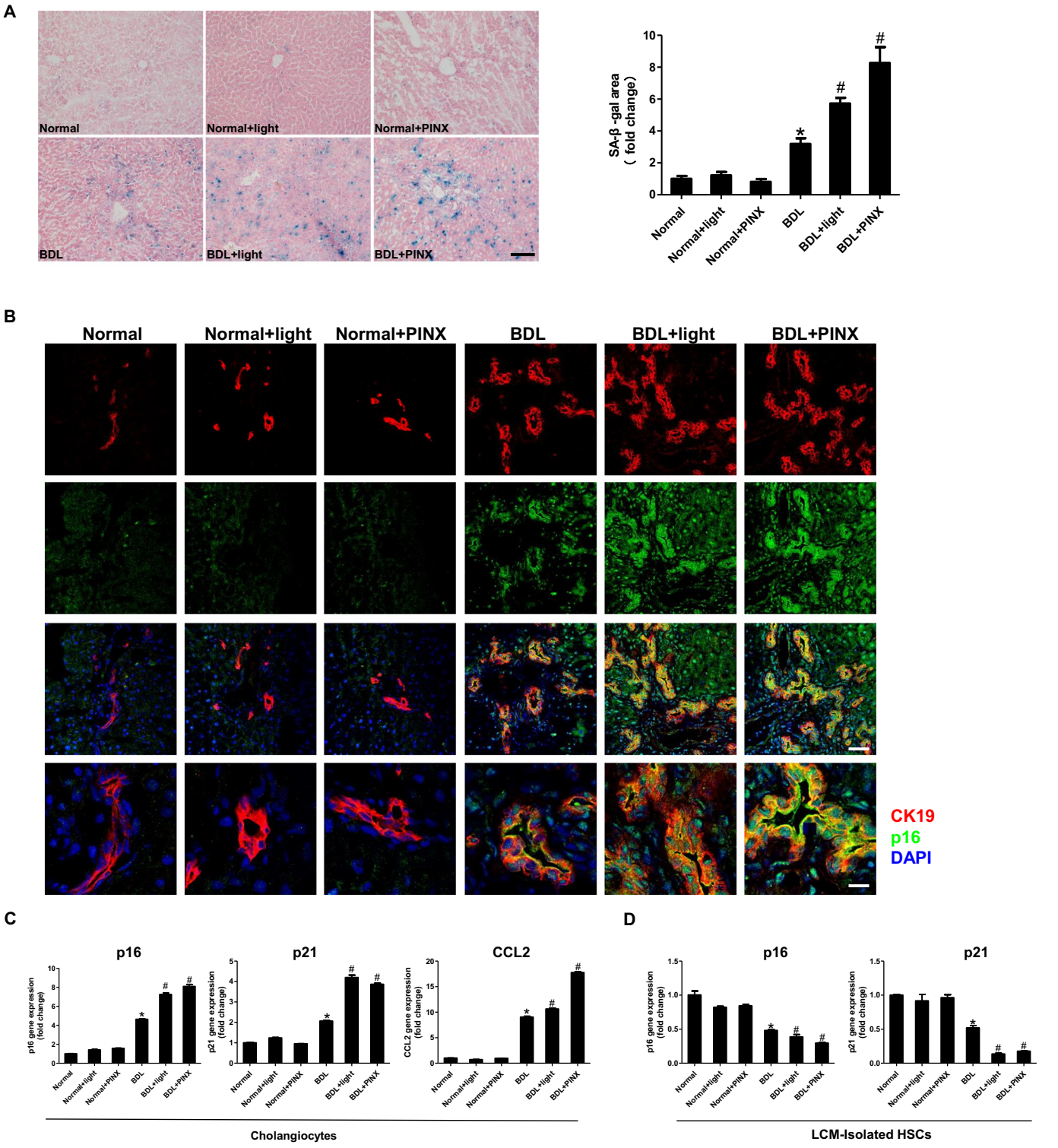


**Fig. 4.** [A] Cellular senescence (by SA-β-gal staining, blue, in liver sections) was enhanced in BDL compared with normal rats and further enhanced in BDL rats following PINX or exposed to light compared with BDL rats (Orig. magn. ×20; scale bar 50 μm). [B] There was increased immunoreactivity of p16 (p16 green, CK19 red) in liver sections of BDL compared with normal rats that was further increased in BDL rats following PINX or exposed to light compared with BDL rats (upper three panels: Orig. magn. ×40, scale bar 50 μm; lower panel: Orig. magn. ×40 zoom5, scale bar 10 μm). [C] There was enhanced mRNA expression of p16, p21, CCL2 in cholangiocytes from BDL rats (compared with normal rats) that was further increased in BDL rats following PINX or exposed to light compared with BDL rats. [D] There was decreased mRNA expression of senescent markers (p16, p21) in LCM-isolated HSC from BDL rats compared with normal rats, which was further decreased in BDL rats following PINX or light treatment compared with LCM-isolated HSC from BDL rats. Data are mean ± SEM of: (i) 10 different fields analyzed from each sample from 3 different animals; (ii) 3 evaluations from 3 cumulative preparations of cholangiocytes from 4 rats; and (iii) 3 evaluations from 3 total liver samples or LCM-isolated HSC from 3 different rats. $^{*}P < 0.05$ vs. Normal; $^{\#}P < 0.05$ vs. BDL.

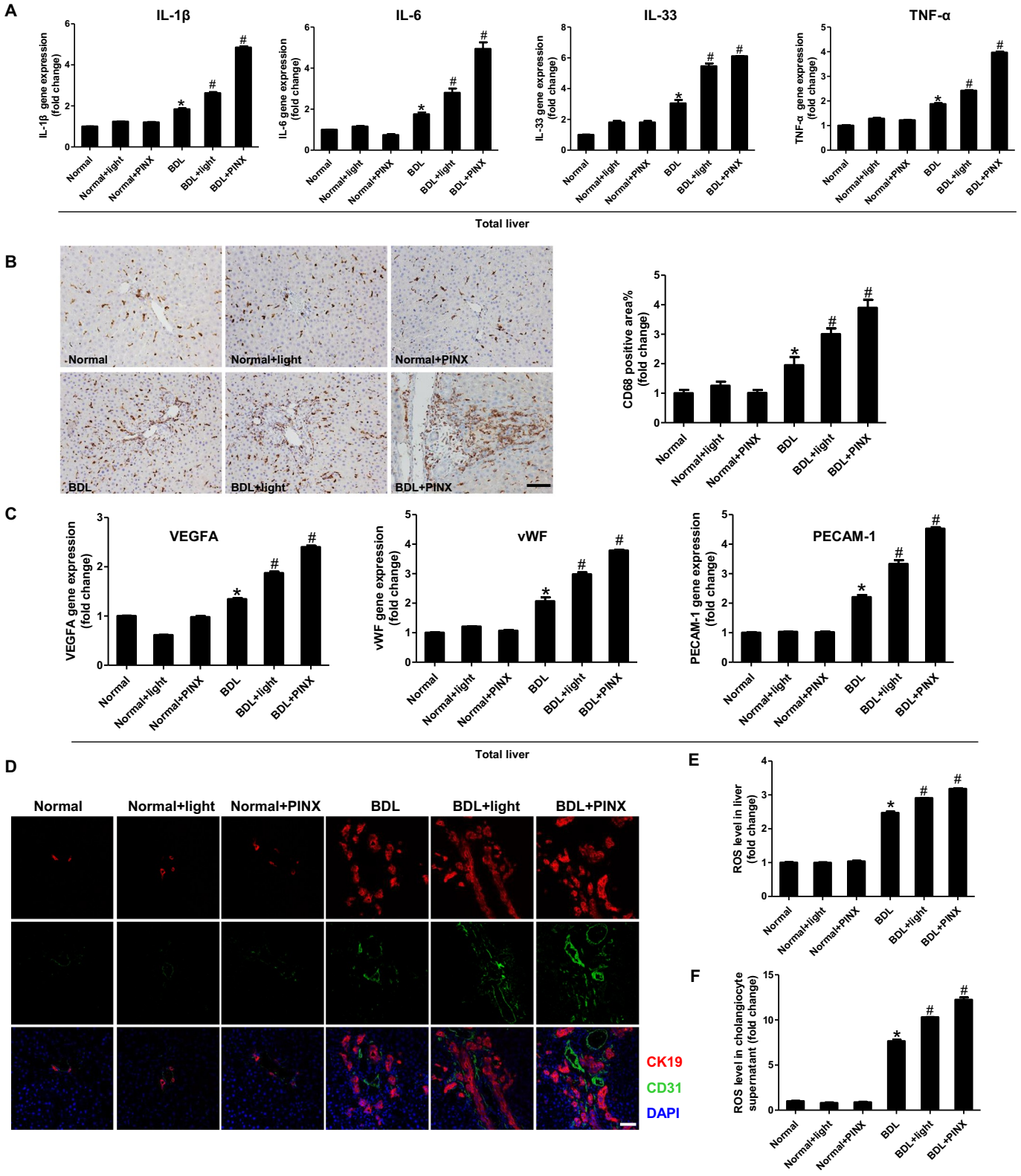


**Fig. 5.** [A] The mRNA expression of IL-1β, IL-6, IL-33, and TNF-α was increased in BDL rats compared with normal rats and further increased in BDL rats following PINX or exposed to light compared with BDL rats. [B] The immunoreactivity of CD68 was increased in liver sections from BDL compared with normal rats and further increased in BDL rats following PINX or exposed to light compared with BDL rats (Orig. magn. ×20; scale bar 50 μm). [C–D] There were increased expression of VEGFA, vWF and PECAM-1 in total liver [C] and immunoreactivity of CD31 (CD31 green, CK19 red) in liver sections [D] (Orig. magn. ×40; scale bar 50 μm) from BDL compared with normal rats that was more increased in BDL rats following PINX or exposed to light compared with BDL rats. [E–F] ROS levels were increased in total liver [E] and cholangiocyte supernatant [F] from BDL rats compared with normal rats and further increased in BDL rats following PINX or prolonged light exposure[E–F]. Data are mean ± SEM of: (i) 10 different fields analyzed from each sample from 3 different animals; (ii) 3 evaluations from 3 total liver samples from 3 different rats; and (iii) 3 evaluations from 3 cumulative preparations of cholangiocyte supernatant from 4 rats. $^{*}P < 0.05$ vs. Normal; $^{\#}P < 0.05$ vs. BDL.

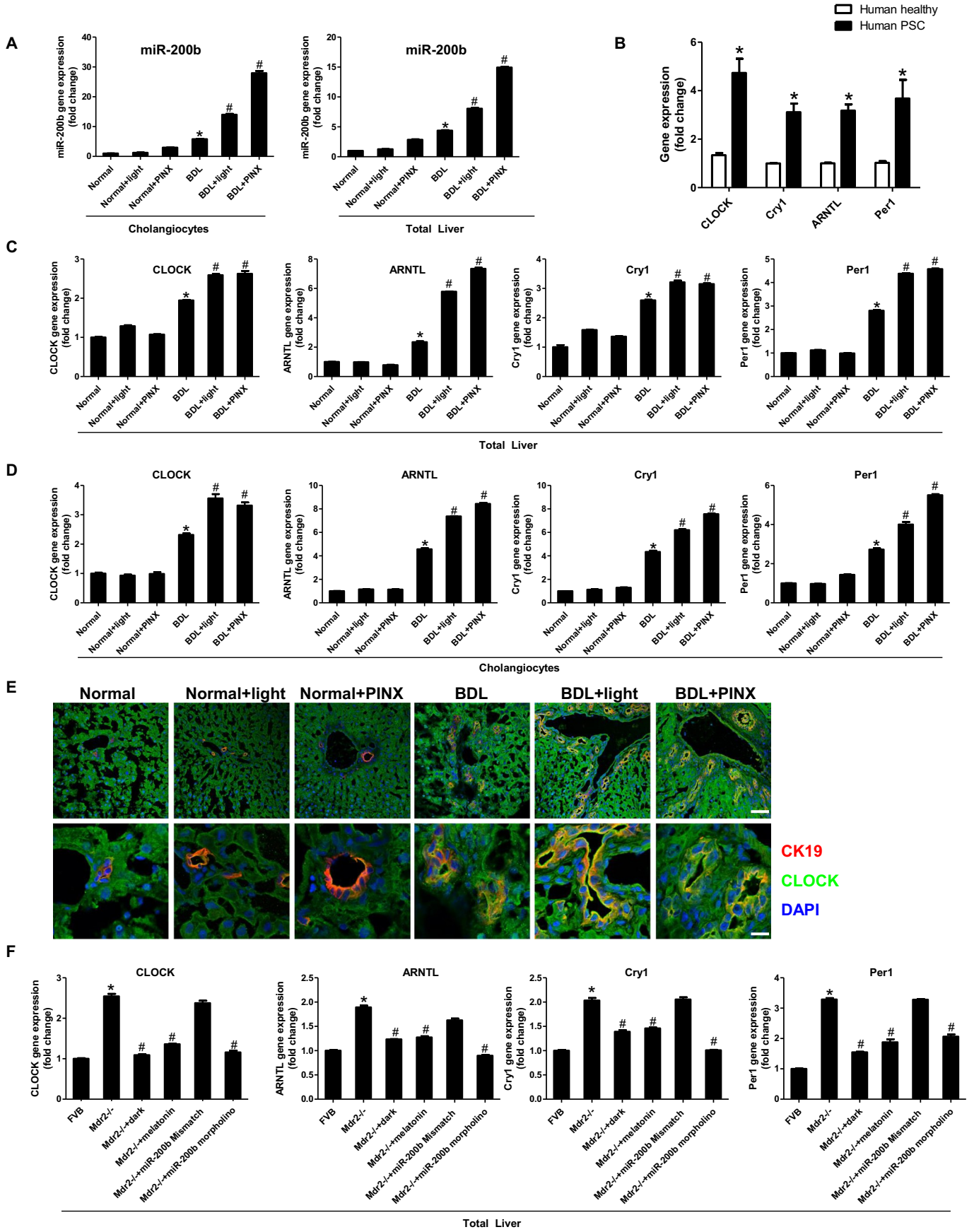


*(caption on next page)*

**Fig. 6.** [A] The mRNA expression of miR-200b was increased in cholangiocytes and total liver from BDL rats compared with normal rats and further enhanced in BDL rats following PINX or prolonged light exposure. [**B**] The mRNA expression of CLOCK, PER1, Cry1, and ARNTL was increased in total liver from late stage PSC patients (n = 5) compared with healthy controls (n = 4), data are mean ± SEM. [C–D] There was increased expression of CLOCK, PER1, Cry1, and BAML1 in total liver [C] and cholangiocytes [D] from BDL rats compared with normal rats that was further increased in BDL rats following PINX or prolonged light exposure compared. [E] Immunofluorescence demonstrated that CLOCK (CLOCK green, CK19 red) immunoreactivity increased in cholangiocytes from BDL compared with normal rats that further increased in cholangiocytes from BDL rats following pinealectomy or prolonged light exposure (upper panel: Orig. magn. ×40, scale bar 50 μm; lower panel: Orig. magn. ×40 zoom5, scale bar 10 μm). [F] There was increased expression of CLOCK, PER1, Cry1, and ARNTL in total liver from Mdr2$^{-/-}$ mice (compared with WT mice) that was reduced by dark exposure or treatment with melatonin or miR-200b inhibitor treatment. Data are mean ± SEM of: (i) 3 evaluations from 3 cumulative preparations of cholangiocytes from 4 rats; and (ii) 3 evaluations from 3 total liver samples from 3 different rats or mice. $^{*}P < 0.05$ vs. the respective control; $^{\#}P < 0.05$ vs. BDL or Mdr2−/−.

### 3.6. Expression of mir-200b and clock genes

The expression of miR-200b (downstream to melatonin and whose expression is increased in Mdr2$^{-/-}$ mice and human PSC samples but decreased by dark exposure or melatonin treatment) [13] was higher in cholangiocytes and total liver from BDL rats but increased in BDL rats following PINX or light exposure compared with BDL rats (Fig. 6A). To determine the specificity of our findings, we confirmed that the expression of miR-200b was decreased in the cholangiocyte line, IMCLs, after treatment with melatonin (Supplementary Fig. 4A). To pinpoint the role of miR-200b in cholangiocyte fibrosis and senescence, we transfected IMCLs with either miR-200b inhibitor or miR-200b mimic (Supplementary Fig. 4A). The expression of fibrosis (TGF-β1, Fn1 and Col1a1) and senescence (p16, p21 and CCL2) genes was decreased in IMCLs treated with melatonin and miR-200b inhibitor but increased in IMCLs treated with miR-200b mimic (Supplementary Fig. 4B–C). Consistent with our previous study showing that administration of melatonin to BDL rats decreases the expression of clock genes [1], we demonstrated that the mRNA expression of the clock genes, CLOCK, Per1, Cry1, and ARNTL was increased in total liver samples (Fig. 6C) and cholangiocytes (Fig. 6D) from BDL rats compared with normal rats, and further enhanced in BDL rats following PINX or light exposure compared with BDL rats (Fig. 6C–D). The mRNA expression of CLOCK, Per1, Cry1, and ARNTL was increased in total liver samples from PSC patients compared with healthy controls (Fig. 6B). There was increased immunoreactivity of CLOCK in liver sections from BDL compared with normal rats, which was further increased in BDL rats following PINX or light treatment compared with BDL rats (Fig. 6E). We also demonstrated enhanced mRNA expression of clock genes in total liver from Mdr2$^{-/-}$ compared with WT mice, which was reduced by prolonged dark exposure or melatonin treatment or in vivo administration of a miR-200b inhibitor (Fig. 6F).

### 3.7. In vitro studies in HIBEpiC, hPSCL and HHStecs

Approximately 99% of hPSCL were CK19 positive (Supplementary Fig. 5A). There was enhanced mRNA expression of AANAT, MT1, MT2, fibrosis genes (Fn1 and TGF-β1), senescence genes (p21 and p16), miR-200b as well as CLOCK, Per1, Cry1 and ARNTL in hPSCL compared with HIBEpiC (Supplementary Fig. 5B–F). We observed increased immunoreactivity of AANAT, MT1 and p16 in hPSCL compared with HIBEpiC (Supplementary Fig. 5G). When HHStecs (that express MT1 and MT2, see Supplementary Fig. 6) were treated with cholangiocyte supernatant from BDL rats, there was increased (i) ROS generation (Fig. 7A–B); (ii) cell proliferation (Fig. 7C–D); (iii) the expression of fibrosis genes (Fig. 7E) compared with HHStecs treated with normal cholangiocyte supernatant. These changes were further increased when HHStecs were treated with cholangiocyte supernatant from BDL rats following PINX or light treatment (Fig. 7A–E). When HHStecs treated with cholangiocyte supernatant from BDL rats there was decreased expression of senescent markers (Fig. 7F) compared with HHStecs treated with normal cholangiocyte supernatant, which was further decreased when HHStecs were treated with cholangiocyte supernatant from BDL rats following PINX or light treatment (Fig. 7F).

## 4. Discussion

We evaluated the effect of PINX and prolonged light exposure (which reduces melatonin serum levels) [3] on BDL-induced biliary damage and liver fibrosis. In BDL rats following PINX or exposed to light there was; (i) decreased melatonin levels in serum and cholangiocyte supernatant and reduced AANAT biliary expression; (ii) increased MT1 but decreased MT2 expression; (iii) increased BDL-induced IBDM, cellular senescence, liver inflammation, liver fibrosis, angiogenesis and TGF-β1 and ROS levels; and (iv) increased expression of melatonin-dependent miR-200b [13] and clock genes in cholangiocytes and total liver. PINX or prolonged exposure to light exacerbates biliary damage and liver fibrosis in cholestatic rats through decreased biliary melatonin synthesis. As validation of our models, we demonstrated that BDL-induced increase in AANAT biliary expression and melatonin levels in serum and cholangiocyte supernatant (likely due to a compensatory mechanism) [1] was reduced in BDL rats following PINX or light exposure. In support of the concept that enhanced biliary damage and liver fibrosis (observed in BDL rats plus PINX or light exposure) is due to reduced expression of melatonin levels, studies have shown reduced melatonin serum levels in rats with PINX [23] and proposed PINX as a model of PBC [27]. The decrease in melatonin synthesis observed in our PINX model is supported by a previous study showing an age-related decline in liver melatonin synthesis [28]. Similarly, prolonged exposure to light increased lipid peroxidation in brain, kidney and liver that was ameliorated by treatment with melatonin [29].

Melatonin exerts its effects by interacting with the G-protein-coupled membrane receptors, MT1, MT2 and MT3 (the latter found only in non-mammals). The increase in the expression in MT1/MT2 in BDL rats (due to a compensatory mechanism associated with enhanced melatonin levels) [1] as well as human PSC cell lines is supported by a study showing enhanced MT1/MT2 expression in cholangiocarcinoma [22]. The increase in MT1 and the decrease in MT2 expression (observed in BDL + PINX or exposed to light) is supported by our preliminary data showing that knock-out of MT1 reduces biliary damage and liver fibrosis, whereas knock-out of MT2 increases biliary senescence and liver fibrosis in cholestatic models [30]. Consistent with a role of biliary senescence (upregulated after PINX) in the downregulation of MT2, a study has demonstrated age-related decline in MT2 expression in rat liver [28]. Supporting our findings, we have demonstrated that melatonin decreases biliary hyperplasia through increased biliary melatonin secretion by interaction with MT1 [2]. To support the concept that downregulation of MT2 induces an increase in biliary damage and liver fibrosis through reduced melatonin synthesis, we have performed studies demonstrating that administration of melatonin to MT2$^{-/-}$ BDL mice presents the increase in biliary damage/senescence and liver fibrosis. Melatonin has been shown to ameliorate liver damage and liver fibrosis as well as systemic oxidative stress in BDL rats and Mdr2$^{-/-}$ mice [13,22,31,32]. Our study provides novel data related to the important protective role of melatonin during biliary damage and liver fibrosis since reduced melatonin levels cause enhanced biliary senescence and liver fibrosis.

A hallmark of liver fibrosis is the activation of HSCs, which serve as major producer of fibrogenic extracellular matrix [33]. Damaged

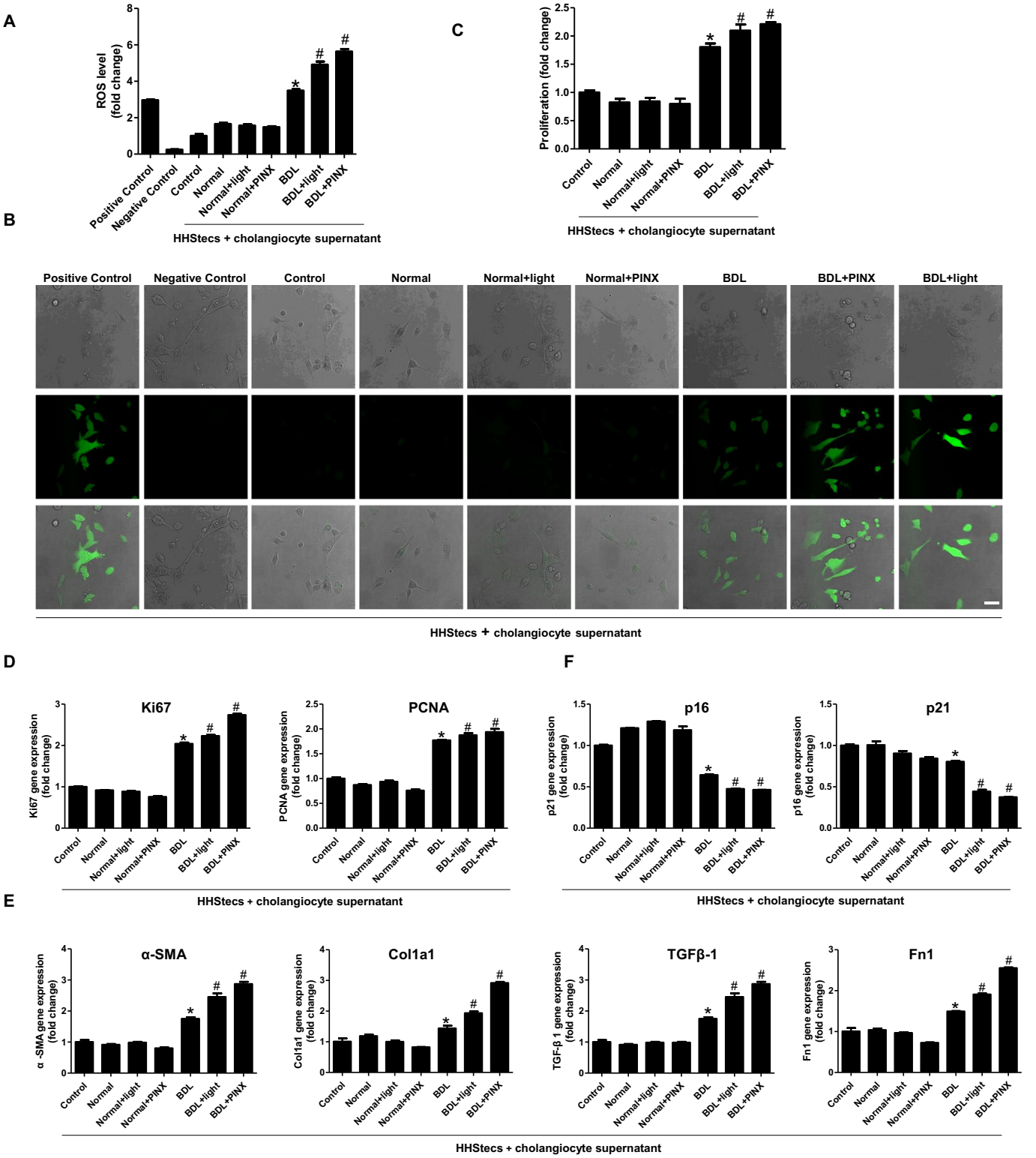


**Fig. 7.** [A–E] There were increased ROS generation [A–B] (Orig. magn. ×20, scale bar 100 μm), cell proliferation [C–D] and expression of fibrosis genes [E] in HHStecs stimulated with cholangiocyte supernatant from BDL rats compared with HHStecs stimulated with cholangiocyte supernatant from normal rats, which were further increased in HHStecs stimulated with cholangiocyte supernatant from BDL rats following PINX or exposed to prolonged light. [F] There was decreased mRNA expression of p16 and p21 in HHStecs treated with cholangiocyte supernatant from BDL rats compared with treated with cholangiocyte supernatant from normal rats, which was further decreased when HHStecs treated were treated with cholangiocyte supernatant from BDL rats following PINX or light treatment. Data are mean ± SEM of the mean for at three independent experiments. $^{*}P < 0.05$ vs. Normal; $^{\#}P < 0.05$ vs. BDL.

cholangiocytes express a number of SASPs (e.g., TGF-β1) [34], profibrogenic and chemotactic proteins, attracting inflammatory cells and activating HSCs by paracrine pathways [6,34]. Parallel to our findings, several studies support melatonin antifibrotic activity [35,36]. Melatonin prevents $H_2O_2$-induced activation of HSCs through regulation of TGF-β1 [36]. Our data expands these studies demonstrating that the

anti-fibrotic effects of melatonin is due not only to interaction with MT1 on HSCs but also to a paracrine mechanism involving enhanced HSCs senescence through decreased release of TGF-β1 and ROS from cholangiocytes. Indeed, we observed increased levels of TGF-β1 and ROS in BDL rats that were further increased in BDL rats + PINX or exposed to light, which likely depends on the decreased melatonin levels leading to increased biliary release of TGF-β1. Supporting this notion, studies have shown that enhanced levels of biliary TGF-β1 not only increase cholangiocyte senescence but also trigger the activation of HSC by a paracrine mechanism [34,37]. Further studies are necessary to determine the direct link between melatonin and TGF-β1, perhaps mediated by changes in miR-200b. In addition to a direct effect of melatonin on melatonin receptor on HSCs, we observed that cholangiocyte supernatant from BDL rats following PINX or prolonged light exposure increased ROS levels that further activate HHStecs. These findings suggest that increased chemotactic factors (likely due to decreased melatonin secretion by cholangiocytes) mediate the activation of HSCs. Supporting our hypothesis and findings, a number of studies have shown that melatonin affects ROS levels in liver cells [10,38]. Also, melatonin protects against alcoholic liver injury through decreased oxidative stress as well as inflammatory responses [10].

Biliary senescence (a hallmark of cholangiopathies) is increased in mouse models of PSC as well as the livers of patients with PSC and PBC [5,9]. Enhanced cholangiocyte senescence and release of SASPs have been shown to trigger the activation of HSCs by paracrine pathways [6,37]. Indeed, there were increased cholangiocyte senescence and decreased cellular senescence of HSCs in BDL rats as well as in HHStecs stimulated with the supernatant of BDL cholangiocytes, which supports our previous finding in cholestatic mice [6]. There is evidence that melatonin loss is linked to senescence, geriatric diseases and thus highlighted the anti-aging effects of melatonin [39]. Recent studies identified melatonin as a novel anti-SASP molecule [40], supporting our finding that the increase of cholangiocyte senescence in BDL rats following PINX or prolonged light exposure is due to reduced melatonin levels. Melatonin possesses a variety of physiological functions including antiangiogenic and anti-inflammatory effects [13,41]. Parallel to a study showing that PINX aggravates acute pancreatitis by increased susceptibility of PINX rats to inflammatory tissue damage [14], we show increased inflammation in BDL rat liver following PINX or light exposure.

A number of studies have shown that angiogenic factors trigger biliary damage and liver fibrosis in cholestatic BDL rats, Mdr2$^{-/-}$ mice as well as human PSC samples, suggesting that modulation of angiogenesis is an important target for the management of liver fibrosis [13,42]. In our study, we show enhanced expression of angiogenic factors and increased angiogenesis in liver from BDL rats, which were further increased in liver from of BDL rats following PINX or light exposure likely due to reduced melatonin levels. Supporting this concept and our finding, melatonin has been shown to exert antiangiogenic activity in Mdr2$^{-/-}$ mice, HepG2 cells and metastatic cancer patients [13,43,44].

A study has shown that: (i) miR-200b is increased in Mdr2$^{-/-}$ mice and human PSC samples; and (ii) melatonin reduces biliary senescence and liver fibrosis through downregulation of miR-200b leading to decreased liver angiogenesis [13]. In this study, we confirmed the expression of miR-200b was increased in rats with PINX and exposed to

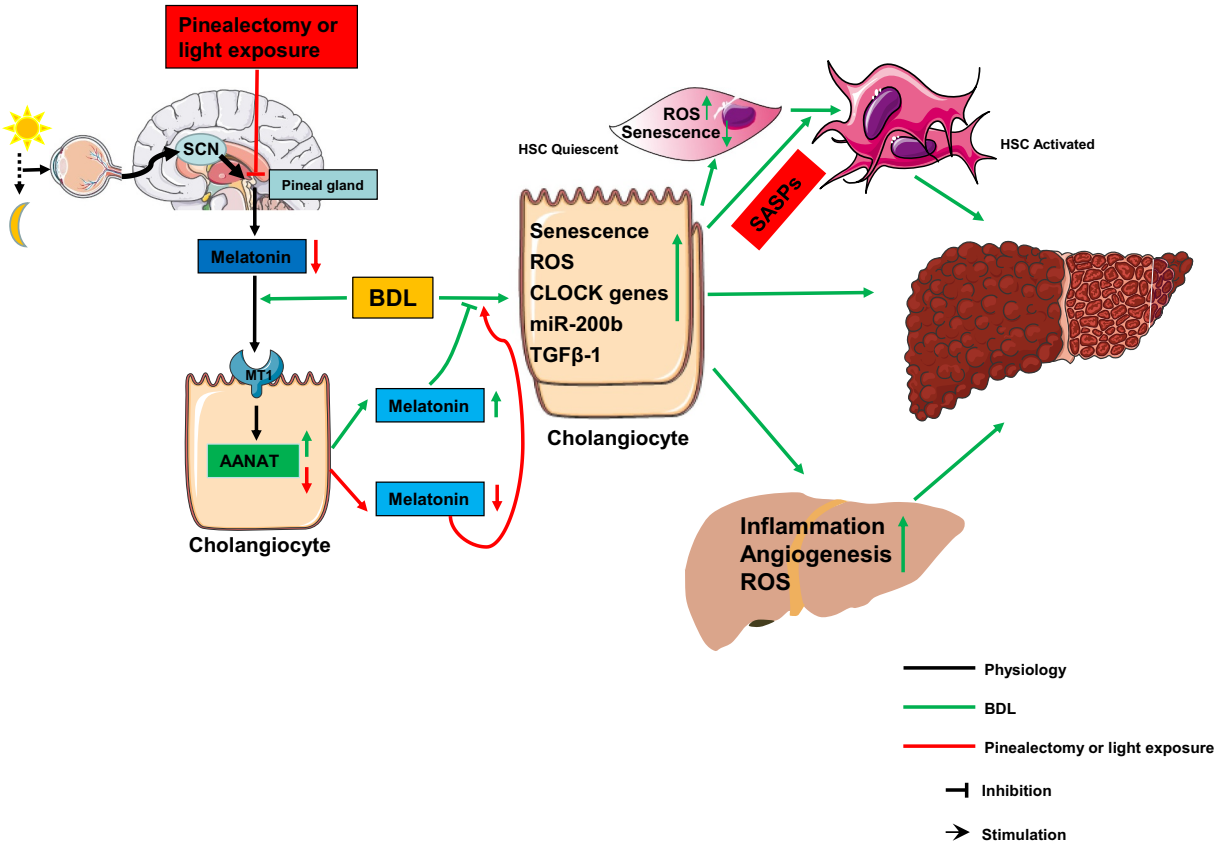


**Fig. 8.** Working model of melatonin regulation of biliary senescence and liver fibrosis during cholestatic liver injury. Melatonin synthesis in the pineal gland is regulated by the light/dark signals detected by the retina. These signals pass through the retino-hypothalamic tract and the superchiasmatic nucleus to the pineal gland, where the melatonin is secreted by pinealocytes. AANAT, the rate-limiting enzyme for melatonin synthesis is also expressed by cholangiocytes. Downregulation of biliary AANAT expression and melatonin secretion by PINX or light exposure exacerbates cholestasis-induced biliary damage and liver fibrosis. Melatonin downregulation of MT1 inhibits cholestasis-induced biliary senescence and liver fibrosis through increased AANAT expression, decreased expression of miR-200b, TGFβ-1 and ROS levels and downregulation of CLOCK genes.

light and in hPSCL and that the enhanced expression of miR-200b was associated with reduced melatonin levels. In support of the notion that melatonin inhibits BDL-induced biliary hyperplasia through downregulation of selected clock genes (upregulated following BDL and in hPSCL) [1], our findings introduce the novel concept that the upregulation of the clock genes, CLOCK, Per1, Cry1 and ARNTL, (due to decreased melatonin levels) trigger the enhanced biliary damage/senescence and liver fibrosis. Opposite to our studies and findings, showing upregulation of clock genes in cholangiocytes from cholestatic animals and downregulation of biliary clock gene expression by melatonin, a number of studies have shown that downregulation of clock genes exacerbates liver injury and fibrosis during cholestasis [45,46]. This discrepancy is likely due to the fact that our studies were performed in pure cholangiocytes [1] but not only in total liver as the other studies have shown [45,46].

Since: (i) melatonin inhibits biliary damage and liver fibrosis by downregulation of miR-200b; and (ii) downregulation of miR-200b (by Vivo Morpholino) in Mdr2$^{-/-}$ mice decreases the expression of selected clock genes, we propose that the modulation of the melatonin/MT1/miR-200b/circadian rhythm may be important top modulate biliary damage and liver fibrosis.

In summary, we demonstrated that PINX or prolonged exposure to light exacerbates biliary damage and liver fibrosis in cholestatic rats by decreased biliary melatonin synthesis (Fig. 8). We propose that the dramatic reduction of melatonin secretion in cholangiocytes during BDL plus PINX or light exposure aggravates biliary damage and liver fibrosis by: (i) increasing biliary senescence through reduced biliary levels of SASPs (e.g., TGFβ-1) and ROS thereby activating of HSCs by a paracrine mechanism; and (ii) directly interacting with MT1 on HSCs.

Supplementary data to this article can be found online at https://doi.org/10.1016/j.bbadis.2019.03.002.

## Transparency document

The Transparency document associated with this article can be found, in online version.

## Financial support

This study was supported by (i) VA Merit Awards (1I01BX003031, HF; 4I01BX000574, GA; 1I01BX001724, FM) from the United States Department of Veteran's Affairs, Biomedical Laboratory Research and Development Service and NIH grants DK054811, DK076898, DK107310, DK110035, DK062975 to GA, SG, FM, DK108959, HF, and DK082435 to SD; (ii) the PSC Partners Grant Award 460933-00001 and Dr. Nicholas C. Hightower Centennial Chair of Gastroenterology from Baylor Scott & White Health (GA); and (iii) Development Service, by University of Rome “La Sapienza” to PO. This material is the result of work supported with resources and the use of facilities at the Central Texas Veterans Health Care System, Temple, Texas. The content is the responsibility of the author(s) alone and does not necessarily reflect the views or policies of the Department of Veterans Affairs or the United States Government.

## Conflict of interest

The authors have declared that no conflict of interest exists.

## References

[1] S. Glaser, E. Gaudio, A. Renzi, R. Mancinelli, Y. Ueno, J. Venter, M. White, S. Kopriva, V. Chiasson, S. DeMorrow, H. Francis, F. Meng, M. Marzioni, A. Franchitto, D. Alvaro, S. Supowit, D.J. DiPette, P. Onori, G. Alpini, Knockout of the neurokinin-1 receptor reduces cholangiocyte proliferation in bile duct-ligated mice, Am. J. Physiol. Gastrointest. Liver Physiol. 301 (2011) G297–G305.

[2] A. Renzi, S. DeMorrow, P. Onori, G. Carpino, R. Mancinelli, F. Meng, J. Venter, M. White, A. Franchitto, H. Francis, Y. Han, Y. Ueno, G. Dusio, K.J. Jensen, J.J. Greene Jr., S. Glaser, E. Gaudio, G. Alpini, Modulation of the biliary expression of arylalkylamine N-acetyltransferase alters the autocrine proliferative responses of cholangiocytes in rats, Hepatology 57 (2013) 1130–1141.

[3] A.J. Lewy, M. Tetsuo, S.P. Markey, F.K. Goodwin, I.J. Kopin, Pinealectomy abolishes plasma melatonin in the rat, J. Clin. Endocrinol. Metab. 50 (1980) 204–205.

[4] D.C. Klein, S. Ganguly, S. Coon, J.L. Weller, T. Obsil, A. Hickman, F. Dyda, 14-3-3 proteins and photoneuroendocrine transduction: role in controlling the daily rhythm in melatonin, Biochem. Soc. Trans. 30 (2002) 365–373.

[5] J.H. Tabibian, C.E. Trussoni, S.P. O'Hara, P.L. Splinter, J.K. Heimbach, N.F. LaRusso, Characterization of cultured cholangiocytes isolated from livers of patients with primary sclerosing cholangitis, Lab. Investig. 94 (2014) 1126–1133.

[6] Y. Wan, F. Meng, N. Wu, T. Zhou, J. Venter, H. Francis, L. Kennedy, T. Glaser, F. Bernuzzi, P. Invernizzi, S. Glaser, Q. Huang, G. Alpini, Substance P increases liver fibrosis by differential changes in senescence of cholangiocytes and hepatic stellate cells, Hepatology. 66 (2017) 528–541.

[7] A. Baghdasaryan, T. Claudel, J. Gumhold, D. Silbert, L. Adorini, A. Roda, S. Vecchiotti, F.J. Gonzalez, K. Schoonjans, M. Strazzabosco, P. Fickert, M. Trauner, Dual farnesoid X receptor/TGR5 agonist INT-767 reduces liver injury in the Mdr2$^{-/-}$ (Abcb4$^{-/-}$) mouse cholangiopathy model by promoting biliary HCO(−)(3) output, Hepatology 54 (2011) 1303–1312.

[8] J.H. Tabibian, S.P. O'Hara, P.L. Splinter, C.E. Trussoni, N.F. LaRusso, Cholangiocyte senescence by way of N-ras activation is a characteristic of primary sclerosing cholangitis, Hepatology 59 (2014) 2263–2275.

[9] L. Meng, M. Quezada, P. Levine, Y. Han, K. McDaniel, T. Zhou, E. Lin, S. Glaser, F. Meng, H. Francis, G. Alpini, Functional role of cellular senescence in biliary injury, Am. J. Pathol. 185 (2015) 602–609.

[10] S. Hu, S. Yin, X. Jiang, D. Huang, G. Shen, Melatonin protects against alcoholic liver injury by attenuating oxidative stress, inflammatory response, and apoptosis, Eur. J. Pharmacol. 616 (2009) 287–292.

[11] H. Wang, W. Wei, N.P. Wang, S.Y. Gui, L. Wu, W.Y. Sun, S.Y. Xu, Melatonin ameliorates carbon tetrachloride-induced hepatic fibrogenesis in rats via inhibition of oxidative stress, Life Sci. 77 (2005) 1902–1915.

[12] A. Cruz, F.J. Padillo, E. Torres, C.M. Navarrete, J.R. Munoz-Castaneda, F.J. Caballero, J. Briceno, T. Marchal, I. Tunez, P. Montilla, C. Pera, J. Muntane, Melatonin prevents experimental liver cirrhosis induced by thioacetamide in rats, J. Pineal Res. 39 (2005) 143–150.

[13] N. Wu, F. Meng, T. Zhou, Y. Han, L. Kennedy, J. Venter, H. Francis, S. DeMorrow, P. Onori, P. Invernizzi, F. Bernuzzi, R. Mancinelli, E. Gaudio, A. Franchitto, S. Glaser, G. Alpini, Prolonged darkness reduces liver fibrosis in a mouse model of primary sclerosing cholangitis by miR-200b down-regulation, FASEB J. 31 (2017) 4305–4324.

[14] J. Jaworek, K. Zwirska-Korczala, J. Szklarczyk, K. Nawrot-Porabka, A. Leja-Szpak, A.K. Jaworek, R. Tomaszewska, Pinealectomy aggravates acute pancreatitis in the rat, Pharmacol. Rep. 62 (2010) 864–873.

[15] I. Susko, S. Alicelebic, E. Cosovic, M. Sahinovic, D. Kapic, S. Custovic, V. Muzika, Gender-related histological changes in the thymus gland after pinealectomy and short-term melatonin treatment in rats, Med Arch. 71 (2017) 385–390.

[16] G. Alpini, R. Lenzi, L. Sarkozi, N. Tavoloni, Biliary physiology in rats with bile ductular cell hyperplasia. Evidence for a secretory function of proliferated bile ductules, J. Clin. Invest. 81 (1988) 569–578.

[17] N. Wu, Y. Han, D. Ray, J. Venter, K. McDaniel, A. Martinez, S. Avila, E. Gaudio, P. Onori, F. Franchitto, F. Meng, M. Guerrier, H. Standeford, G. Alpini, S. Glaser, Knockdown of the melatonin receptor, MT2, enhances biliary hyperplasia and liver fibrosis in cholestatic bile duct ligated (BDL) mice: novel evidence for a hepato-protective role of MT2, Hepatology 60 (2014) A410.

[18] M. Ishhi, B. Vroman, N.F. LaRusso, Isolation and morphologic characterization of bile duct epithelial cells from normal rat liver, Gastroenterology. 97 (1989) 1236–1247.

[19] S. De Minicis, E. Seki, H. Uchinami, J. Kluwe, Y. Zhang, D.A. Brenner, R.F. Schwabe, Gene expression profiles during hepatic stellate cell activation in culture and in vivo, Gastroenterology. 132 (2007) 1937–1946.

[20] L.A. Coelho, R. Peres, F.G. Amaral, R.J. Reiter, J. Cipolla-Neto, Daily differential expression of melatonin-related genes and clock genes in rat cumulus-oocyte complex: changes after pinealectomy, J. Pineal Res. 58 (2015) 490–499.

[21] A.K. Trivedi, S. Malik, S. Rani, V. Kumar, Pinealectomy abolishes circadian behavior and interferes with circadian clock gene oscillations in brain and liver but not retina in a migratory songbird, Physiol. Behav. 156 (2016) 156–163.

[22] Y. Han, P. Onori, F. Meng, S. DeMorrow, J. Venter, H. Francis, A. Franchitto, D. Ray, L. Kennedy, J.F. Greene, A. Renzi, R. Mancinelli, E. Gaudio, S. Glaser, G. Alpini, Prolonged exposure of cholestatic rats to complete dark inhibits biliary hyperplasia and liver fibrosis, Am. J. Physiol. Gastrointest. Liver Physiol. 307 (9) (2014) G894–G904, https://doi.org/10.1152/ajpgi.00288.2014.

[23] G.A. Bubenik, G.M. Brown, Pinealectomy reduces melatonin levels in the serum but not in the gastrointestinal tract of rats, Biol. Signals 6 (1997) 40–44.

[24] M. Dumont, V. Lanctôt, R. Cadieux-Viau, J. Paquet, Melatonin production and light exposure of rotating night workers, Chronobiol. Int. 29 (2012) 203–210.

[25] P.H. McGuinness, D. Painter, S. Davies, G.W. McCaughan, Increases in intrahepatic CD68 positive cells, MAC387 positive cells, and proinflammatory cytokines (particularly interleukin 18) in chronic hepatitis C infection, Gut. 46 (2000) 260–269.

[26] L. Liu, Z. You, H. Yu, L. Zhou, H. Zhao, X. Yan, D. Li, B. Wang, L. Zhu, Y. Xu, T. Xia, Y. Shi, C. Huang, W. Hou, Y. Du, Mechanotransduction-modulated fibrotic microniches reveal the contribution of angiogenesis in liver fibrosis, Nat. Mater. 16 (2017) 1252–1261.

[27] S.C. Cunnane, M.S. Manku, D.F. Horrobin, The pineal and regulation of fibrosis: pinealectomy as a model of primary biliary cirrhosis: roles of melatonin and prostaglandins in fibrosis and regulation of T lymphocytes, Med. Hypotheses 5 (1979)

403–414.
[28] M. Sanchez-Hidalgo, J.M. Guerrero Montavez, P. Carrascosa-Salmoral Mdel, C. Naranjo Gutierrez, P.J. Mdel, C.A. de la Lastra Romero Lardone, Decreased MT1 and MT2 melatonin receptor expression in extrapineal tissues of the rat during physiological aging, J. Pineal Res. 46 (2009) 29–35.
[29] G. Baydas, E. Ercel, H. Canatan, E. Donder, A. Akyol, Effect of melatonin on oxidative status of rat brain, liver and kidney tissues under constant light exposure, Cell Biochem. Funct. 19 (2001) 37–41.
[30] N. Wu, T. Kyritsi, P. Invernizzi, J. Venter, F. Bernuzzi, F. Meng, K. Sato, E. Gaudio, H. Francis, T. Zhou, P. Onori, A. Franchitto, G. Alpini, S. Glaser, Differential impact of MT1 and MT2 melatonin receptor deletion on biliary proliferation, senescence, and liver fibrosis during cholestatic liver injury, Hepatology. 66 (2017) A330.
[31] V. Tahan, R. Ozaras, B. Canbakan, H. Uzun, S. Aydin, B. Yildirim, H. Aytekin, G. Ozbay, A. Mert, H. Senturk, Melatonin reduces dimethylnitrosamine-induced liver fibrosis in rats, J. Pineal Res. 37 (2004) 78–84.
[32] M. Esrefoglu, M. Gul, M.H. Emre, A. Polat, M.A. Selimoglu, Protective effect of low dose of melatonin against cholestatic oxidative stress after common bile duct ligation in rats, World J. Gastroenterol. 11 (2005) 1951–1956.
[33] V. Hernandez-Gea, S.L. Friedman, Pathogenesis of liver fibrosis, Annu. Rev. Pathol. 6 (2011) 425–456.
[34] T. Zhou, N. Wu, F. Meng, J. Venter, T.K. Giang, H. Francis, K. Kyritsi, C. Wu, A. Franchitto, D. Alvaro, M. Marzioni, P. Onori, R. Mancinelli, E. Gaudio, S. Glaser, G. Alpini, Knockout of secretin receptor reduces biliary damage and liver fibrosis in Mdr2(−/−) mice by diminishing senescence of cholangiocytes, Lab. Investig. 98 (11) (2018) 1449–1464, https://doi.org/10.1038/s41374-018-0093-9.
[35] S. Shajari, A. Laliena, J. Heegsma, M.J. Tunon, H. Moshage, K.N. Faber, Melatonin suppresses activation of hepatic stellate cells through RORalpha-mediated inhibition of 5-lipoxygenase, J. Pineal Res. 59 (2015) 391–401.
[36] J. Gu, L. Zhuang, G.C. Huang, Melatonin prevents H2O2-induced activation of rat hepatic stellate cells, J. Pineal Res. 41 (2006) 275–278.
[37] N. Wu, F. Meng, P. Invernizzi, F. Bernuzzi, J. Venter, H. Standeford, P. Onori, M. Marzioni, D. Alvaro, A. Franchitto, E. Gaudio, S. Glaser, G. Alpini, The secretin/secretin receptor axis modulates liver fibrosis through changes in transforming growth factor-beta1 biliary secretion in mice, Hepatology. 64 (2016) 865–879.
[38] N. Das, A. Mandala, S. Naaz, S. Giri, M. Jain, D. Bandyopadhyay, R.J. Reiter, S.S. Roy, Melatonin protects against lipid-induced mitochondrial dysfunction in hepatocytes and inhibits stellate cell activation during hepatic fibrosis in mice, J. Pineal Res. 62 (2017).
[39] R. Hardeland, Melatonin and the theories of aging: a critical appraisal of melatonin's role in antiaging mechanisms, J. Pineal Res. 55 (2013) 325–356.
[40] S. Yu, X. Wang, P. Geng, X. Tang, L. Xiang, X. Lu, J. Li, Z. Ruan, J. Chen, G. Xie, Z. Wang, J. Ou, Y. Peng, X. Luo, X. Zhang, Y. Dong, X. Pang, H. Miao, H. Chen, H. Liang, Melatonin regulates PARP1 to control the senescence-associated secretory phenotype (SASP) in human fetal lung fibroblast cells, J. Pineal Res. 63 (2017).
[41] J.R. Colares, E.G. Schemitt, R.M. Hartmann, F. Licks, M.D. Soares, A.D. Bosco, N.P. Marroni, Antioxidant and anti-inflammatory action of melatonin in an experimental model of secondary biliary cirrhosis induced by bile duct ligation, World J. Gastroenterol. 22 (2016) 8918–8928.
[42] E. Gaudio, B. Barbaro, D. Alvaro, S. Glaser, H. Francis, Y. Ueno, C.J. Meininger, A. Franchitto, P. Onori, M. Marzioni, S. Taffetani, G. Fava, G. Stoica, J. Venter, R. Reichenbach, S. DeMorrow, R. Summers, G. Alpini, Vascular endothelial growth factor stimulates rat cholangiocyte proliferation via an autocrine mechanism, Gastroenterology. 130 (2006) 1270–1282.
[43] E.J. Sohn, G. Won, J. Lee, S. Lee, S.H. Kim, Upregulation of miRNA3195 and miRNA374b mediates the anti-angiogenic properties of melatonin in hypoxic PC-3 prostate cancer cells, J. Cancer 6 (2015) 19–28.
[44] P. Lissoni, F. Rovelli, F. Malugani, R. Bucovec, A. Conti, G.J. Maestroni, Anti-angiogenic activity of melatonin in advanced cancer patients, Neuro Endocrinol Lett. 22 (2001) 45–47.
[45] P. Chen, Z. Han, P. Yang, L. Zhu, Z. Hua, J. Zhang, Loss of clock gene mPer2 promotes liver fibrosis induced by carbon tetrachloride, Hepatol. Res. 40 (2010) 1117–1127.
[46] P. Chen, X. Kakan, S. Wang, W. Dong, A. Jia, C. Cai, J. Zhang, Deletion of clock gene Per2 exacerbates cholestatic liver injury and fibrosis in mice, Exp. Toxicol. Pathol. 65 (2013) 427–432.